

THE ADDITIONAL LINE COMPONENT WITHIN IRON K α PROFILE IN MCG-6-30-15: EVIDENCE FOR BLOB EJECTION?JIAN-MIN WANG¹, JIN-LU QU¹ & SUI-JIAN XUE²*Accepted for Publication in The Astrophysical Journal*

ABSTRACT

The *EPIC* data of MCG-6-30-15 observed by *XMM-Newton* were analyzed for the complexities of the iron K α line. Here we report that the additional line component (ALC) at 6.9 keV undoubtedly appears within the broad iron K α line profile at high state whereas it disappears at low state. These state-dependent behaviors exclude several possible origins and suggest an origin of the ALC in matter being ejected from the vicinity of the black hole. At the low state, the newborn blob ejected from the accretion disk is so Thomson thick that hard X-ray is blocked not to ionize the old ones, leading to the disappearance of the ALC. When the blob becomes Thomson thin due to expansion, the hard X-ray will penetrate it and ionize the old ones, emitting the ALC at the high state. The blob ejection is a key to switch on/off the appearance of the ALC.

Subject headings: galaxies: active - galaxies: Seyfert: individual: MCG-6-30-15

1. INTRODUCTION

MCG-6-30-15 (redshift $z = 0.00775$, Fisher et al. 1995) is an ideal laboratory in the sky to test how to accrete matter onto a supermassive black hole. The profile of the iron K α line as a key probe to the general relativistic effects have provided an essential clue to understand the details of the gas dynamics and radiation mechanism around the black hole. It has been recognized (see a recent review of Reynolds & Nowak 2003): 1) the strong general relativistic redshifts (including Doppler effects) (Tanaka et al. 1995; Fabian et al. 1995; Fabian et al. 2002; Turner et al. 2002; Fabian et al. 2003; Vaughan & Fabian 2004); 2) energy extraction from the spinning black hole (Blandford & Znajek 1977; Wilms et al. 2001; Fabian et al. 2002).

The complexities within the iron K α line profile have been shown by the appearance of several narrow components. The 6.4 keV narrow component quite often appears in Seyfert 1 galaxies (Yaqoob et al. 2000). Turner et al. (2002) show evidence for the narrow components in NGC 3516, indicating the gravity-controlled redshifts. Evidence for an absorption edge at 8.7 keV has been found in Mrk 766, suggesting the presence of ejecta moving at a velocity of 15000 km/s (Pounds et al. 2003). The long time *XMM-Newton* observations (~ 325 ks) unambiguously presented an additional line component (ALC) at 6.9 keV (Fabian et al. 2002; Fabian & Vaughan 2003). It is very interesting that the ALC did not appear in the observation of 108th revolution (Wilms et al. 2001). However, the origin of the ALC remains open. How does this component appear? Is it related to the blob ejection from the vicinity of supermassive black hole?

The above questions are the main goals of the present paper. We show that the ALC is state-dependent on 2.5-10keV X-ray flux in MCG-6-30-15. This strongly implies it may link with blob ejection from the accretion disk.

2. SPECTRAL ANALYSIS AND RESULTS

Three sets (revolution 301, 302, 303) of MOS and pn data were taken from the *XMM-Newton Science Archive*. We re-analyzed the data for the properties of the ALC with the standard SAS pipeline and XSPEC. Following Fabian et al.

(2002), the spectral responses used in the present paper were `m1_medv9q19t5r5_all_15.rsp` for MOS-1 (and similarly for MOS-2) and `epn_sw20_sdY9_medium.rmf` for the pn in the present paper. As argued by Fabian et al. (2002) and Fabian & Vaughan (2003), “there remain problems with the model for charge transfer inefficiency for pn small-window mode data” and “it is not clear whether the MOS or the pn data give a more accurate description of the shape of the broad iron line”. Both MOS and pn data were therefore analyzed in the present paper. It is found that the final results are in agreement with each other quantitatively. We give a detail description of MOS data reduction.

The low and high states for pn data are distinguished by a critical count rate $R_{pn} = 16$ cts/s in Fabian et al. (2002). This corresponds to a MOS count rate $R_{MOS} = 6$ cts/s as shown by the MOS-1/2 light curves in Figure 1. The pn light curves have been given in Fabian et al. (2002). During the observations of *XMM-Newton*’s orbit 108, the 2-10keV fluxes were just at the low state (Wilms et al. 2001). The spectra at the high and low states were produced, respectively. We noted that MCG-6-30-15 was in a high state for a large fraction of the period in orbit 301, 302, 303, but the length (~ 130 ks) at the low state is long enough for our goals. The final results of the present work are not very sensitive to the critical count rates R_{MOS} and R_{pn} .

The spectra were fitted with XSPEC by the following models: 6.4keV narrow component, Compton reflection model, `Laor` profile (Laor 1991) and a Gaussian profile of the ALC. In Laor’s model, the emissivity of iron K α line is assumed $\propto R^{-k}$, where R is the radius of the disk and k is the index. The hydrogen column density is fixed at $N_H = 4.06 \times 10^{20} \text{cm}^{-2}$ (Dickey & Lockman 1990). The inclination angle of the disk (i) was fixed at 28.4° , and the iron abundance is 3 solar as in Fabian et al. (2002) at both the low and high states. At the low state, the best fit without the 6.9 keV component is given in Table 1. The errors are quoted at the 90% confidence level. Including this component gave a slightly poorer fit ($\chi^2 = +0.1$), excluding the presence of the ALC at the low state. The upper limits for the equivalent width and luminosity are also given in Table 1. At the high state, $\chi^2 = -15.9$ was obtained with a significance larger than 99% after we added 6.9 keV ALC. The ALC width

¹ Laboratory for High Energy Astrophysics, Institute of High Energy Physics, The Chinese Academy of Sciences, Beijing 100039, P.R. China

² National Observatories of China, The Chinese Academy of Sciences, Beijing 100020, P.R. China

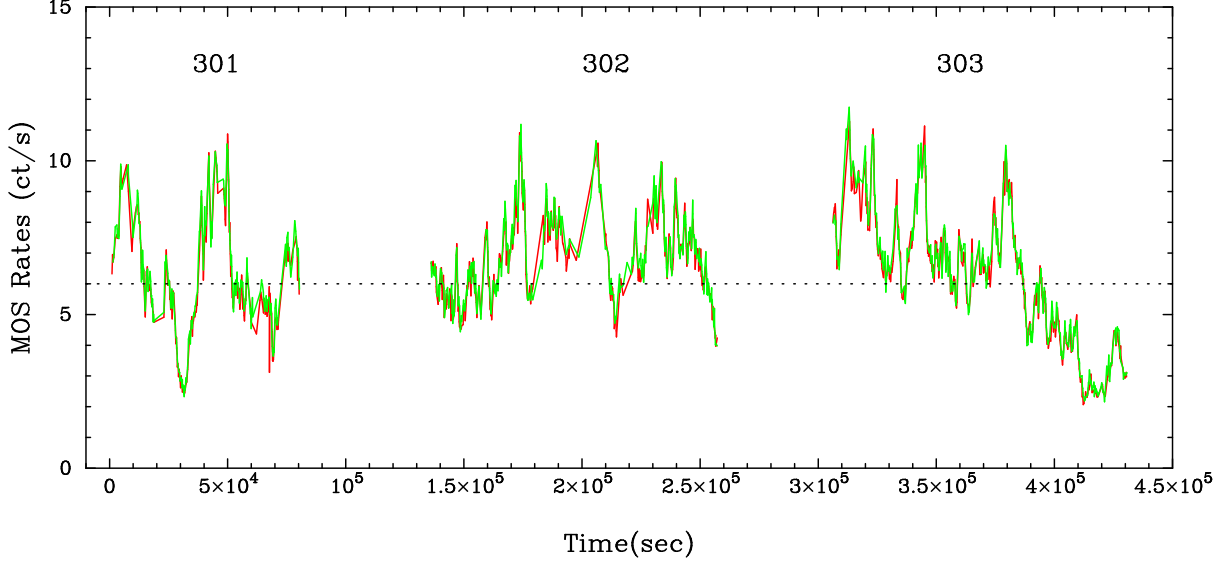


FIG. 1.— The light curves of MCG-6-30-15 by 325ks *XMM-Newton* observations. The red curve is MOS-1 data and green MOS-2 data.

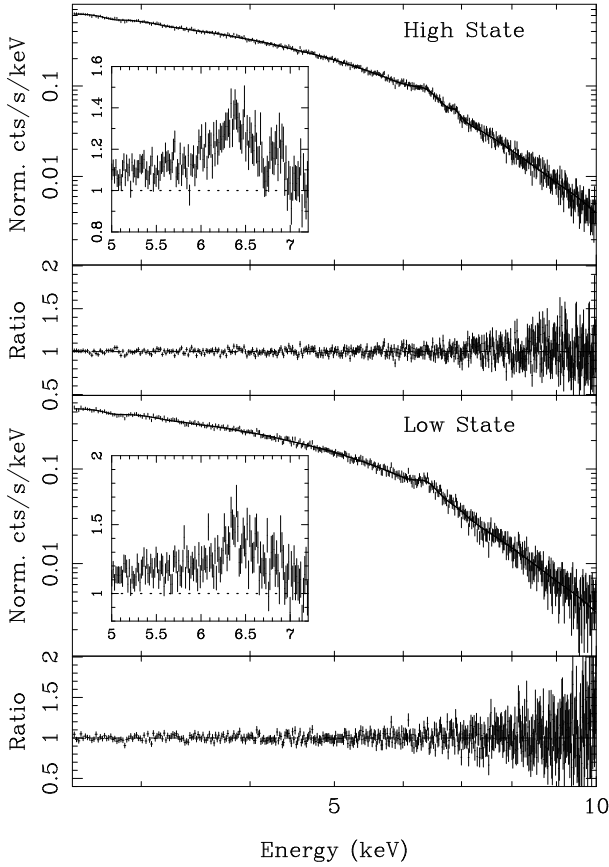


FIG. 2.— The combined MOS spectrum (addspect is used to add the MOS-1/2 spectra) at the low (lower panel) and the high states (upper panel). The insert panels show a close-up of the ratio of the data to the model (the Galactic absorption plus a single power law in 2.5-3.0 and 7.5-10 keV) around the iron line region. It is clearly showed that the ALC appears at the high state whereas it disappears at the low state.

is consistent with zero, but has an upper limit 70eV from pn data. We have done the F -test to find the significance of the ALC changes from the low state to the high state. We found that the statistic value $F = 5.69$ and the probability $p = 7.82 \times 10^{-4}$

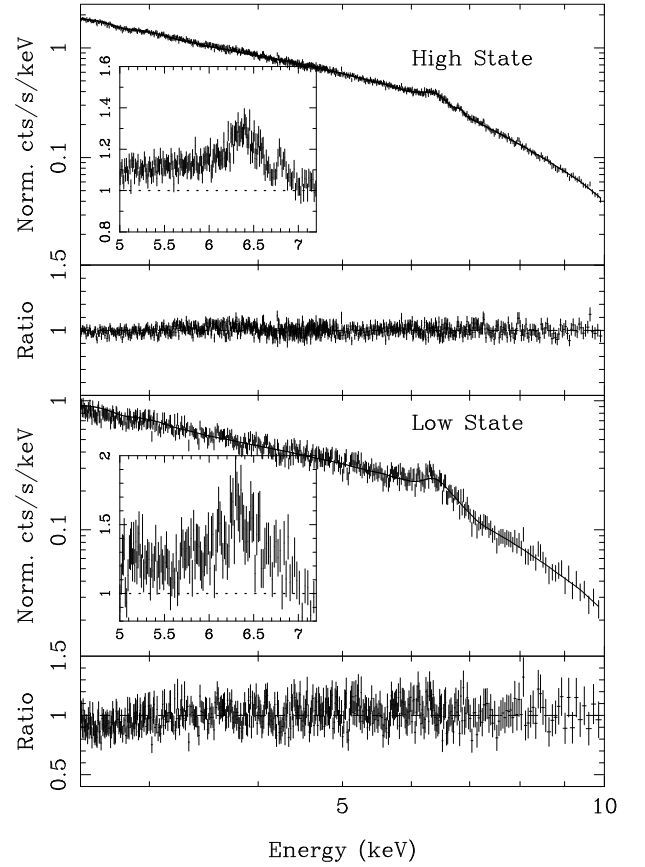


FIG. 3.— The same as in Fig. 2, but for the combined pn spectrum.

(the significance is $1 - p$). Though the upper limit of the ALC EW at the low state is close to the lower limit of EW at the high state, the difference in luminosity of the ALC between the high and low state shows the variability of the ALC. The best fittings are shown by Figure 2 for MOS-1/2 data. It is quite sure that the ALC appears at the high state and disappears at the low state.

The same procedures have been done for the pn data. Figure 3 shows the pn data and the best fitting. The results are given in

TABLE 1 THE RESULTS OF FITS TO THE COMBINED MOS-1/2 AND PN DATA

States		MOS-1/2		pn data	
		High	Low	High	Low
ALC	E_A (keV)	$6.86^{+0.03}_{-0.29}$	6.9 (fixed)	$6.81^{+0.05}_{-0.01}$	6.9 (fixed)
	EW (eV)	$19.5^{+7.5}_{-3}$	< 12.0	$20.0^{+4.4}_{-3.0}$	< 11.0
	(eV)	$3.0^{+3.44}_{-3}$	$3.0^{+6.6}_{-3.0}$...
	L_{ALC}^1	0.85 0.33	< 0.41	0.83 0.18	< 0.35
Broad K	E (keV)	$6.28^{+0.09}_{-0.48}$	$6.98^{+0.16}_{-0.34}$	$6.32^{+0.03}_{-0.09}$	$6.60^{+0.01}_{-0.12}$
	EW (eV)	239^{+81}_{-30}	453^{+60}_{-67}	256 19	499^{+40}_{-80}
	k	3.48 0.16	$4.30^{+0.23}_{-0.53}$	3.15 0.08	3.73 0.02
	r_{in}	$1.99^{+0.31}_{-0.76}$	$1.78^{+0.19}_{-0.54}$	$2.85^{+0.14}_{-0.19}$	$1.40^{+0.08}_{-0.17}$
Narrow K	EW (eV)	89 10	80 18	43.7 5.3	106^{+7}_{-19}
	(eV)	176^{+31}_{-25}	137^{+84}_{-49}	133 25	170.0^{+80}_{-50}
Continuum		1.83 0.01	$1.77^{+0.03}_{-0.02}$	2.03 0.01	$1.89^{+0.04}_{-0.05}$
	Fluxes ²	3.17	2.32	3.28	2.42
χ^2_{dof}		454.8/488	436.1/489	479.0/571	249.6/319

Note: upper limit

¹ The ALC luminosity in unit of 10^{40} ergs/s ($q_0 = 0.5$ and $H_0 = 75$ km s⁻¹ Mpc⁻¹ are used)² The flux is in 2.5-10 keV in the unit of 10^{-11} erg cm⁻² s⁻¹.

Table 1. We found the EW of the ALC at the high state is obviously stronger than that at the low state. The narrow 6.4 keV component shows a significant change in pn data, especially at the high state, it becomes weaker. The central energy of the broad K line in pn data at the low state is lower than that in MOS data, but we should note that the error bar of MOS data is larger than that of pn data. We found that the results of pn data are quite similar to that of MOS.

From Table 1, the broad K line is enhanced at the low state whereas it is weakened at the high state. This property is generally consistent with a long ASCA observation (Iwasawa et al. 1996). The ALC has an opposite response of the iron K line to the continuum. An extensive analysis of iron K line has been made in Fabian & Vaughan (2003). They found two-component model can explain the variability of iron K line: a constant (or less variable) component and a highly variable power-law component. They suggest that the less variable component drives the variability of the K line. It remains open whether there is a relation between the highly variable power-law component and the ALC. We will investigate this issue in future.

It has been noted that the central energy of the broad K line shifts to $6.98^{+0.16}_{-0.34}$ keV in MOS data, which perhaps overlaps with the ALC. The ALC could be thus hidden by the broad K line at the low state. We relaxed the ALC energy to explore whether it shifts from the high to low states, but we did not get any significantly improved results. The XSPEC fitting only presents the upper limits for its equivalent and zero width as seen in Table 1. It is very difficult to separate this component, but the fact should be robust that the ALC intrinsically weakens (significantly) or disappears at the low state. Though the current MOS data does not allow us to separate the ALC from the broad iron K line at the low state, the pn data clearly shows the broad K line does not overlap the ALC. The properties of the ALC set strong constraints on its origins.

3. ORIGINS OF THE ALC

In this section we explore possible originations of the ALC based on the state-dependent properties. Fabian et al. (2002) ruled out the origin in strong iron-L absorption by comparing

with soft X-ray spectrum (Lee et al. 2001). Here we exclude others and suggest that the ALC originate from the matter being ejected from the vicinity of the black hole.

First, recombination lines from a cooling optically thin plasma blobs ejected from the nucleus (Wang et al. 2000a, Turner et al. 2002, Fabian et al. 2002) unlikely appears as the additional line component. The K recombination line luminosity is $L_K = (4 - 3)R_p^3 n_e^2 \epsilon_K$ from a hot plasma with radius R_p and number density n_e , where ϵ_K is the emissivity of the K line. The Thomson depth is $\tau_{es} = n_e R_p \sigma_{Th}$, we have $L_K = (4 - 3) \epsilon_K R_p^2 \tau_{es}^{-2} \sigma_{Th}^{-2}$, where σ_{Th} is the Thomson cross section. For iron hydrogen-like atomic ions, the highest emissivity $\epsilon_K = 1.4 \times 10^{-24}$ A_{Fe} of Fe XXVI 1.78 A, Fe XXV 1.84 A, Fe XXV 1.86 A etc. (Raymond & Smith 1977), the dimension of the hot plasma

$$R_p \approx 7.5 \times 10^{16} L_{K,40}^{-1/2} \tau_{es,-1}^{-1} A_{Fe}^{-1} \text{ (cm)}; \quad (1)$$

and number density

$$n_e \approx 2.0 \times 10^6 L_{K,40}^{-1/3} \tau_{es,-1}^{-3/2} A_{Fe}^{-1/2} \text{ (cm}^{-3}\text{)}; \quad (2)$$

are required, where $\tau_{es} = 0.1 \tau_{es,-1}$, $L_{K,40} = L_K / 10^{40}$ erg/s and A_{Fe} is iron abundance in unit of sun. Thomson depths should be $\tau_{es} > 0.1$, otherwise the recombination line will be greatly broadened by Comptonization inside the hot plasma (Pozdnyakov et al. 1979). The cooling timescale of hot plasma is of

$$t_{ff} \approx 30.0 L_{K,40} T_8^{1/2} \tau_{es,-1}^{-3/2} A_{Fe}^{-1/2} \text{ (yr)}; \quad (3)$$

Such a long timescale implies that the recombination line should be constant within at least the observational interval (~ 300 ks). The ALC should be independent to the states of 2-10 keV fluxes. This directly conflicts with the observed properties of the ALC. Moreover, if it were the recombination line due to the cooling plasma, as a constant line emission, it should be enhanced at the low state and weakened at the high state since a constant line flux becomes stronger in an underlying weak continuum. The disappearance of this component at the low state does not favor this origination. We note that absorption will be harder to detect at the low state, but more importantly, the warm absorber could well be less ionized in the low state, leaving no

absorption. In order to rule out variability of the absorber, the RGS data should be investigated in future.

Second, it is implausible that the ALC originate from a region of disk photoionized by a flare likely due to a magnetic field reconnection as suggested for NGC 3516 (Turner et al. 2002). A multiwavelength study of MCG-6-30-15 showed $\text{FWHM(H)} = 2400 \pm 200 \text{ km/s}$, luminosity at 5100 Å, $L(5100 \text{ Å}) = 2.53 \times 10^{42} \text{ erg/s}$ and the bolometric luminosity $L_{\text{bol}} = 4.0 \times 10^{43} \text{ erg/s}$ (Reynolds et al. 1997). The size of the broad line region of H is $R_{\text{BLR}} = 2.51 \text{ lt-d}$ from the empirical reverberation mapping relation $R_{\text{BLR}} = 32.9 L(5100 \text{ Å})^{1/4} \text{ lt-d}$ (Kaspi et al. 2000). The mass of the black hole in MCG-6-30-15 is then estimated $M_{\text{BH}} = (2.1 \pm 0.3) \times 10^6 M_{\odot}$ from the virial formulation $M_{\text{BH}} = 1.5 \times 10^5 (R_{\text{BLR}}/\text{lt-d}) \text{ FWHM(H)}^2 M_{\odot}$. The analysis of *XMM-Newton* light curves showed $M_{\text{BH}} = 10^6 M_{\odot}$ for the accordance with the break frequency $f_{\text{br}} = 10^{-4} \text{ Hz}$ in its power spectrum (Vaughan et al. 2003), which is in good agreement with that from empirical reverberation relation. We thus have the accretion rate $\dot{m} = \dot{M}/\dot{M}_{\text{Edd}} = 0.14$, where $\dot{M}_{\text{Edd}} = 1.3 \times 10^{24} m_6^{-1} (\text{g/s})$, $m_6 = M_{\text{BH}}/10^6 M_{\odot}$, and the accretion efficiency $\eta = 0.1$. For the simplicity, we still use the standard accretion model to estimate the parameters of the iron K line region (Novikov & Thorne 1973).

A necessary condition of the ionization parameter $\xi = 500$ is required for a photoionized plasma on disk by flares to emit 6.9 keV, where $\xi = 4 \pi R^2 F_X / n_H$, F_X is the ionizing X-ray flux and n_H the hydrogen density (Matt, Fabian & Ross 1993). We assume a conversion efficiency (χ) of gravitational energy into X-ray, and have $F_X = \chi F$, where $F = 3M_{\text{BH}} \dot{M} f(R) / (8 R^3)$ is the flux of the dissipated gravitational energy and $f(R)$ is the general relativistic correction (Novikov & Thorne 1973). This condition gives a critical radius for a flare $r_c = 16.2 \frac{2-9}{-1} \frac{2-9}{\chi} (\approx 500)^{2-9} \dot{m}_{-1}^{2-3}$ (in the units of $R_G = GM_{\text{BH}}/c^2$) from the standard disk, where the viscosity of the disk $\eta = 0.1$ and $\dot{m}_{-1} = \dot{m}/0.1$. The parameter χ is generally thought to be close to the unit in corona model (Haardt & Maraschi 1991). This critical radius is insensitive to the parameters η and χ . The width of a line emitted at the radius r_c is given by $\Delta E = E \sin \theta = (2r_c)^{1/2}$ for a Schwarzschild black hole (Gerbal & Pelat 1981), where θ is the viewing angle, giving a minimum width of 0.58 keV for $\theta = 28^\circ$. This width is much broader than the observed. Thus the origin of the ALC in a highly ionized plasma by a large flare on the disk should be ruled out.

Additionally, the Doppler shift due to Keplerian rotation around a Schwarzschild black hole (or far away from its center of a Kerr black hole) might give rise to the appearance of the ALC. The Lorentz factor and velocity of Keplerian rotation are given by $\gamma = [(r-2)/(r-3)]^{1/2}$ and $\beta = (r-2)^{-1/2}$ in the unit of light speed (see eq.5.4.4a,b on page 423 in Novikov & Thorne 1973). Then the Doppler factor reads $D = (r-3)^{1/2} (r-2)^{-1/2} \sin^{-1}$ for approaching and receding direction (Novikov & Thorne 1973), respectively. If the 6.9 keV line is due to Doppler blue shift from 6.4 keV, it corresponds to a radius $r = 22.4$ for $\theta = 28^\circ$. The timescale of Keplerian rotation is $t_{\text{Kep}} = 1.0 \times 10^3 m_6 (r=10)^{3/2} \text{ sec}$. The length of the present observations has several hundred orbits of the Keplerian rotation. Symmetrically there should be an emission line at 5.56 keV due to Doppler redshift. We added a Gaussian

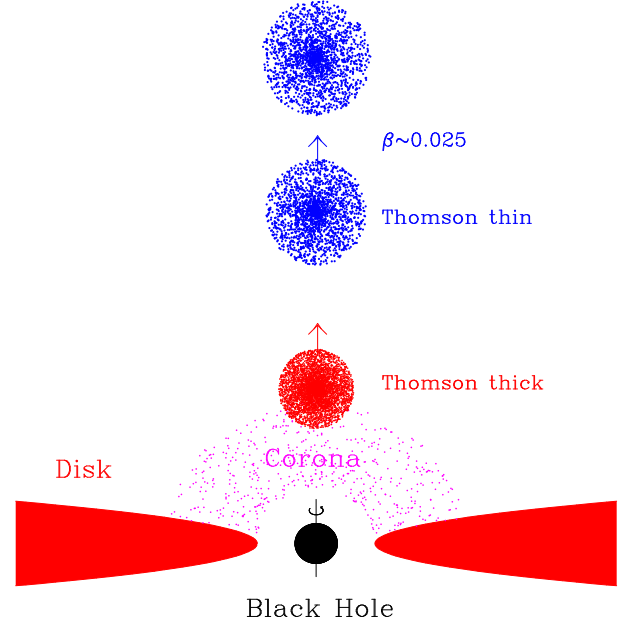


FIG. 4.— The illustrating model proposed in this paper. The newborn blob ejected from the vicinity of SMBH is Thomson thick, which prevents the old blobs from the hard X-ray of the corona. The ALC then disappears at the low state. The magnetic field pressure inside the blob drives the blob to expand and become Thomson thin after a period $\sim 10^4 \text{ sec}$. The hard X-ray can penetrate the blobs, which are emitting the ALC at the high state. The velocity of the ejected blobs is $\beta = v/c = 0.025$. The figure is not scaled.

line at 5.56 keV to test the plausible existence of this pair line, we found a very slight improvement $\chi^2 = -0.01$. Such a line does not appear in the current observational data. The situation in MCG-6-30-15 is thus quite different from the case in NGC 3516, which shows two pairs of narrow emission lines around 6.4 keV due to Doppler shifts (Turner et al. 2002).

Finally, we have to consider the possibility of origin in the ejected blobs from the vicinity of SMBH based on the state-dependent behavior of the ALC.

There is some direct evidence for blob ejection to take place at the low state in 3C 120 (Marscher et al. 2002), and microquasars (Livio et al. 2003). The ejected clouds are suggested for the 8.7 keV absorption edge in Mrk 766, but the ejection mechanisms are highly uncertain (Pounds et al. 2003). In a new model of jet formation, the transients of the accretion disk is due to jet production. The disk is at the low state when the blob ejection takes place there. The transition is caused by most likely a large scale magnetic (Livio et al. 2003), which can be produced by the disk dynamo (Tout & Pringle 1996). The angular momentum transportation, production of the large scale magnetic field and blob ejection are entangled with each other. As a consequence of the angular momentum conservation, the ejected blob may whirl around the black hole spin axis. This would result in more complicate and sophisticated effects. This is beyond the scope of the current data. We do not discuss this further in the present paper. The following is devoted to an outline of the model of blob's evolution to explain the observation.

We introduce a ratio $q = \dot{M}_{\text{eje}}/\dot{M}$, the fraction of the ejection to the accretion rate of the disk. The value of q is highly unknown, but it should be a significant fraction of the accretion rate estimated from the observations. In the case of MCG-6-30-15, we have a very crude estimate of $q = 1 - F_{\text{low}}^X / F_{\text{high}}^X = 0.2$

from the Table 1. The ejection lasts a period of the low state t (Marscher et al. 2002; Livio et al. 2003). We assume that the ejected blob has an initial radius $R_{b,0} = r_{b,0} R_G$, the density of the blob is $\rho_0 = M_b / \frac{4}{3} R_{b,0}^3$, where $M_b = M_{\text{eje}} t = q M t$. The Thomson depths of the newborn blob is given by $\tau_{\text{es},0} = \rho_0 R_{b,0}$, namely,

$$\tau_{\text{es}} = 4.69 \times 10^2 q_{-1} \underline{m}_{-1} t_4 r_b^{-2} m_6^{-1}; \quad (4)$$

where electron scattering opacity $\tau_{\text{es}} = 0.34$, $q_{-1} = q/0.1$, and $t_4 = t/10^4 \text{ sec}$. Such a Thomson thick blob will block the X-ray to illuminate the blobs, which have been ejected before this newborn blob. The ALC from the ejected blobs will be quenched at the low state.

However, the magnetic field pressure inside the newborn blob is driving it to expand. The expanding velocity can be roughly estimated by $\frac{1}{2} \dot{b}^2 = B^2/8$, we have

$$\dot{b} = 7.5 \times 10^7 B_4 r_0^{-1/2} m_6 (\tau_{\text{es}} = 500)^{1/2} \text{ (cm s}^{-1} \text{)}; \quad (5)$$

where the magnetic field $B_4 = B/2.5 \times 10^4 \text{ G}$ (the equipartition value). The ejection velocity of the blob can be estimated $v_{\text{eje}} = 0.025c$ from the Doppler blue shift $D_{\text{max}} = 6.86/6.71/0.23$ for the viewing angle $\theta = 28.4^\circ$. The sub-relativistic velocity is consistent with the very weak radio emission in MCG-6-30-15 (Ulvestad & Wilson 1984). The opening angle of the blobs will be $\theta_b = R_b/H_b = v_{\text{eje}}/0.1$, where H_b is the distance of the ejected blob from the black hole. The ionization parameter of the ejected blobs outside the corona is given by

$$\xi = 1.1 \times 10^2 \dot{b}_{b,0.1} L_{X,42} h_{b,\beta}^{-1} m_6^{-1} \tau_{\text{es}}^{-1}; \quad (6)$$

where $h_{b,\beta} = H_b/10^3 R_G$ and $\dot{b}_{b,0.1} = \dot{b}/0.1$. Setting $\tau_{\text{es}} = 500$, we found a critical height

$$H_b^c = R_G = 2.21 \times 10^2 \tau_{\text{es}}^{-1} L_{X,42} \dot{b}_{b,0.1}; \quad (7)$$

above which the iron is emitting $6.4 - 6.7 \text{ keV}$ K line and below which iron ions are fully ionized. We obtained another critical height of the blob,

$$H_b^{\text{es}} = R_G = 2.17 \times 10^2 \tau_{\text{es}}^{-1} (q_{-1} \underline{m}_{-1})^{1/2} t_4^{1/2} m_6^{-1/2}; \quad (8)$$

when the Thomson depth $\tau_{\text{es}} = 1$. It is found that $H_b^c > H_b^{\text{es}}$. This implies that it is the time for the ejected blob to emit iron K line when the Thomson depth of the blob becomes thin. The newborn blob then switches on X-ray to ionize the old blobs, leading to a recurrence of the ALC. The proposed model is illustrated in Figure 3. The fluorescent K line luminosity from one ejected blob is given by (Krolik & Kallman 1987),

$$L_K = 2.34 \times 10^{39} \frac{2}{b_{b,0.1}} A_{\text{Fe},\beta} \tau_{\text{es}} \text{ (erg s}^{-1} \text{)}; \quad (9)$$

where the optical depth of the K edge $\tau_K = 2.0 A_{\text{Fe},\beta} \tau_{\text{es}}$, $A_{\text{Fe},\beta} = A_{\text{Fe}}/3$, the mean fluorescent yield $Y = 0.6$, the observed X-ray spectrum is used as the illuminating source $L_* = 4.1 \times 10^{41} (\tau_K)^{-0.83} \text{ erg s}^{-1} \text{ keV}^{-1}$ at the high state, and line energy $E_K = 6.7 \text{ keV}$. The observed ALC luminosity is of $8.5 \times 10^{39} \text{ erg s}^{-1}$, which needs about 4 blobs.

The lifetime of the ejected blob is estimated by $\tau_{\text{es}} = 0.01 \tau_{\text{es},2}$ due to expansion when the blob contributes less to the observed ALC. It yields the final radius $R_b = R_G = 2.17 \times 10^2 (q_{-1} \underline{m}_{-1})^{1/2} (t_4 m_6)^{1/2} \tau_{\text{es},2}^{-1/2}$ from equation (4), implying a lifetime $t_{\text{blob}} = R_b/\dot{b}$, i.e.

$$t_{\text{blob}} = 5.0 \times 10^5 B_4^{-1} r_{b,0}^{1/2} \tau_{\text{es},2}^{-1/2} \text{ (sec)}; \quad (10)$$

The typical lifetime is long enough to observe the process that the newborn blob switches on/off the old blobs to emit the ALC.

The proposed model focuses on the ALC behaviors, but the ejected blobs are undergoing acceleration by radiation pressure and the ionization parameter is changing (Chelouche & Netzer 2001). A detail model of blobs undergoing a magnetic field-driven expansion is in preparation.

A Gaussian profile of the ALC is assumed in the present paper. Thermal broadening is quite small ($E/E_0 = 4.3 \times 10^{-4} T_6^{0.5}$, where $T_6 = T/10^6 \text{ K}$, then $E = 3 \text{ eV}$ at the ALC energy $E = 6.9 \text{ keV}$ for a 10^6 K plasma). The profile of the iron K line from the ejected blobs is mainly controlled by several other factors: 1) velocity distribution of the ejected blob which may be influenced by the interaction between the blob and its surroundings (for example, the medium of wind from the disk); 2) redshift due to gravity of the black hole in the center; 3) the changes of ionization degrees of the blobs with distance from the center. The detail profiles of a line from the jet around a black hole has been done by Wang et al. (2000b). However the present EPIC data poorly gives the information on the detail profile of the ALC.

Interestingly, Pounds et al. (2003) found an absorption at 8.7 keV in Mrk 766, which shifts with flares. This implies the line-of-sight absorption in Mrk 766. They suggest a 'cloud' (ejected from the disk) model for this absorption and predict an emission feature significantly contributed at 6.7 keV . Most recently, Turner et al. (2003) found a narrow component at 5.7 keV in Mrk 766, suggesting the emission from the decelerated blobs (Wang et al. 2000a). The pn data do not show absorption edge feature above 8.0 keV at both the low and high states in MCG-6-30-15. The case in MCG-6-30-15 may be different from Mrk 766. These features should be investigated in future.

It should be mentioned that a highly Doppler blueshifted Fe K emission line appeared in two quasars PKS 2149-306 (Yaqoob et al. 1999) and CXOCDFS J033225.3-274219 (Wang et al. 2003). PKS 2149-306 is a radio-loud quasar and the jet has a velocity of $0.75c$. The later has a velocity of $0.6 - 0.7c$. The jets in the two objects have much faster velocities than the blob's in MCG-6-30-15. If the model for the ALC suggested is correct in the present paper, it would be of interests in what reason is responsible for the difference of the ejection velocities. A future study on the comparison of MCG-6-30-15 with the two quasars might shed light on this difference. We need further observations with higher energy resolution and longer monitoring time to probe the physical processes taking place around the supermassive black hole.

4. CONCLUSIONS

We show in the present work that the appearance of the ALC depends on the states of the source. At the low state, this component disappears whereas it appears clearly at the high state. We argue that this state-dependent behaviors of ALC strongly indicate the origin in the blobs ejected from the innermost region of the accretion disk. A simple model for the state-dependent behaviors of the ALC has been outlined in this paper. The newborn blob is initially Thomson thick and switches off the X-ray from hot corona to ionize the old blobs, giving rise to the ALC disappears. With expansion of the newborn blob driven by the magnetic field, it becomes Thomson thin and switches on X-ray to ionize the blob and then ALC appears. Future mission, such as *Astro-E II*, may resolve the detail (profile and possible different components) of the ALC with high energy resolution. This would help to explore the origin of the ALC and its implications. Additionally, monitoring MCG-6-

30-15 is desired to test variabilities of the ALC and the relation with the continuum so as to understand the process of the blob ejection. This process is an intermediate state between relativistic radio jets and the large outflow velocities observed in Seyfert galaxies. It is believed that the X-ray emission lines would trace the processes of the blob ejection.

The authors acknowledge a referee for the careful and helpful comments significantly improving the paper. J.M.W. is grateful to T. J. Turner, S. Komossa, R. Staubert and K. Werner for interesting discussion. S.M. Jia and Y. Chen are greatly thanked for their help in *XMM* data reduction. This research is financed by the Special Funds for Major State Basic Research Projects and supported by Grant for Distinguished Young Scientist from NSFC.

REFERENCES

- Blandford, R. D. & Znajek, R. L., 1977, *MNRAS*, 179, 343
 Chelouche, D. & Netzer, H., 2001, *MNRAS*, 326, 916
 Dickey, J.M. & Lockman, F.J., 1990, *ARAA*, 28, 215
 Fabian, A.C. et al., 2002, *MNRAS*, 335, L1
 Fabian, A. C.; Nandra, K.; Reynolds, C. S.; Brandt, W. N.; Otani, C.; Tanaka, Y.; Inoue, H.; Iwasawa, K., 1995, *MNRAS*, 277, L11
 Fabian, A. C.; Rees, M. J.; Stella, L.; White, N. E., 1989, *MNRAS*, 238, 729
 Fabian, A.C. & Vaughan, S., 2003, *MNRAS*, 340, L28
 Fisher, K. B.; Huchra, J. P.; Strauss, M. A.; Davis, M.; Yahil, A.; Schlegel, D., 1995, *ApJS*, 100, 69
 Gerbal, D. & Pelat, D., 1981, *A&A*, 95, 18
 Haardt, F. & Maraschi, L., 1991, *ApJ*, 380, L51
 Iwasawa, K., et al. 1996, *MNRAS*, 282, 10381
 Kaspi, S.; Smith, P. S.; Netzer, H.; Maoz, D.; Jannuzi, B. T.; Givon, U., 2000, *ApJ*, 533, 631
 Krolik, J.H. & Kallman, T.R., 1987, *ApJ*, 320, L5
 Laor, A., 1991, *ApJ*, 376, 90
 Livio, M., Pringle, J. & King, A.R., 2003, *ApJ*, 593, 184
 Marscher, A.P., et al., 2002, *Nature*, 417, 625
 Matt, G.; Fabian, A. C.; Ross, R. R., 1993, *MNRAS*, 262, 179
 Mewe, R., 1999, in *X-ray Spectroscopy in Astrophysics*, ed. J.van Paradijs & J.A.M. Bleeker, Springer, Berlin, p139
 Novikov, N.I. & Thorne, K.S., 1973, *Black Holes*, eds. de Witt, C & de Witt, B., Gordon & Breach, New York
 Pounds, K.A.; Reeves, J. N.; Page, K. L.; Wynn, G. A.; O'Brien, P. T., 2003, *MNRAS*, 342, 1147
 Pozdniakov, L. A.; Sobol, I. M.; Sunyaev, R. A., 1979, *A&A*, 75, 214
 Raymond, J. C. & Smith, B. W., 1977, *ApJS*, 35, 419
 Reynolds, C.S. & Nowak, M., 2003, *Phys. Rept.*, 377, 389
 Reynolds, C. S.; Ward, M. J.; Fabian, A. C.; Celotti, A., 1997, *MNRAS*, 291, 403
 Sako, M., Kahn, S.M., Branduardi-Raymont, G., Kaastra, J.S., Brinkman, A.C., Page, M.J., Behar, E., Paerels, F., Kinkhabwala, A., Liedahl, & den Herder, J.W., 2003, *ApJ*, 596, 114
 Shakura, N. I. & Sunyaev, R. A., 1973, *A&A*, 24, 337
 Tanaka, Y., Hayashida, K.; Iwasawa, K.; Kii, T.; Kunieda, H.; Makino, F.; Matsuoka, M., 1995, *Nature*, 375, 659
 Tout, C.A. & Pringle, J., 1996, *MNRAS*, 281, 219
 Turner, T.J., et al., 2002, *ApJ*, 574, L123
 Turner, T.J., Kraemer, S.B. & Reeves, J.N., 2003, *ApJ*, astro-ph/0310885
 Ulvestad, J. S. & Wilson, A. S., 1984, *ApJ*, 285, 439
 Vaughan, S. & Fabian, A. C., 2004, *MNRAS*, astro-ph/0311473
 Vaughan, S., Fabian, A.C. & Nandra, K., 2003, *MNRAS*, 339, 1237
 Wang, J.-M., Yuan, Y.-F., Wu, M., & Kusunose, M., 2000a, *ApJ*, 541, L41
 Wang, J.-M., Zhou, Y.-Y., Yuan, Y.-F., Cao, X. & Wu, M., 2000b, *ApJ*, 544, 381
 Wang, J., et al., 2003, *ApJ*, 590, L87
 Wilms, J.; Reynolds, C. S.; Begelman, M. C.; Reeves, J.; Molendi, S.; Staubert, R.; Kendziorra, E., 2001, *MNRAS*, 328, L27
 Yaqoob, T., et al., 1999, *ApJ*, 525, L9
 Yaqoob, T., Goerge, I.M. & Turner, T.J., 2002, in "High Energy Universe at Sharp Focus: Chandra Science", eds. S. Vrtilek, E.M. Schlegel, L. Kuhi., p203